ICES
CIEM

International Council for
the Exploration of the Sea

Conseil International pour
l'Exploration de la Mer

Poleward spawning of Atlantic mackerel (*Scomber scombrus*) is facilitated by ocean warming but triggered by energetic constraints

T. C. dos Santos Schmidt [1,2,*], A. Slotte [2], A. H. Olafsdottir [1], L. Nøttestad [2], T. Jansen [3,4], J. A. Jacobsen [5], S. Bjarnason [1], S. M. Lusseau[4], K. Ono [2], S. Hølleland [2,6], A. Thorsen [2], A. B. Sandø [2], and O. S. Kjesbu [2]

[1]Marine and Freshwater Research Institute, Fornubúðir 5, IS-220 Hafnarfjöður, Iceland
[2]Institute of Marine Research, P.O. Box 1870 Nordnes, 5817 Bergen, Norway
[3]Greenland Institute of Natural Resources, Kivioq 2, PO Box 570, 3900 Nuuk, Greenland
[4]National Institute of Aquatic Resources (DTU-Aqua), Kemitorvet, 2800 Kgs. Lyngby, Denmark
[5]Faroe Marine Research Institute, P.O. Box 3051. Nóatún 1. FO-110 Tórshavn, Faroe Islands
[6]Norwegian School of Economics, Helleveien 30, 5045 Bergen, Norway

* *Corresponding author: (354) 7906633;* e-mail: thassya.dos.santos.schmidt@hafogvatn.is.

The Northeast Atlantic mackerel is an income breeder with indeterminate fecundity, spawning in multiple batches at optimal temperatures around 11°C in the upper water column during February–July along the continental shelf from 36–62°N. Based on macroscopic staging of gonads (N ~62000) collected in 2004–2021, we detected an on-going extension of spawning activities into the Norwegian Sea feeding area (62–75°N), reaching stable levels around 2012 onwards. This poleward expansion increased as more fish entered the area, whilst the maximum proportions of spawners concurrently dropped from about 75 to 15% from May to July. Detailed histological examinations in 2018 confirmed the macroscopic results but clarified that 38% of the spawning-capable females in July terminated their spawning by atresia. We suggest that increased access to suitable spawning areas (≥10°C), following ocean warming from 2002 onwards, functions as a proximate cause behind the noticed expansion, whereas the ultimate trigger was the historic drop in body growth and condition 10 years later. Driven by these energetic constraints, mackerel likely spawn in the direction of high prey concentrations to rebuild body resources and secure the future rather than current reproduction success. The ambient temperature that far north is considered suboptimal for egg and larval survival.

Keywords: condition factor, global warming, histology, macroscopic maturity, Northeast Atlantic mackerel, spawning extension, stock size.

Introduction

Climate variability impacts the ecology of fish populations in myriads of ways mediated via changes in abundance, phenology, and geographical distribution (Poloczanska *et al.*, 2016; Fogarty *et al.*, 2017; Fernandes *et al.*, 2020; Wang *et al.*, 2020). Ocean warming may, for instance, promote longer migrations of warm-temperate species, especially pelagic ones, but may also negatively affect the body growth and fecundity of cold-temperate species (Cheung *et al.*, 2009; Pörtner and Peck, 2010; Poloczanska *et al.*, 2016). Poleward (latitudinal) shifts can be considered as one of the key mechanisms to counteract or diminish any detrimental effect of higher temperatures on spawning behaviour (Shoji *et al.*, 2011; Sandø *et al.*, 2020) and the produced embryos (Alix *et al.*, 2020). Collectively, these complex life-history responses affect species fitness but also, eventually, fisheries and management (Astthorsson *et al.*, 2012; Boyd *et al.*, 2020). Poleward expansions for several fish species have been observed in the North Atlantic over the last couple of decades (Kjesbu *et al.*, 2014; Sundby *et al.*, 2016; Baudron *et al.*, 2020). Northeast Atlantic (NEA) mackerel (*Scomber scombrus*; hereafter generally mackerel) appears as an obvious study object in this respect, firstly due

to its reproductive ecology and secondly due to its temperature preferences, as specified in the next paragraphs.

The reproductive ecology of mackerel is highly complex, both because of the exceedingly broad latitudinal coverage but also because of the reproductive style. Currently, this stock is distributed from Morocco (30°N) to Svalbard (78°N) and undertakes seasonal migration between spawning, feeding, and overwintering areas (Trenkel *et al.*, 2014; Berge *et al.*, 2015). Mackerel has a long spawning season, traditionally spawning from January/February outside the Portuguese coast and Cadiz, moving northwards until June/July in southern areas of the Nordic Seas (Cunningham *et al.*, 2007; Jansen *et al.*, 2013; Trenkel *et al.*, 2014; ICES, 2021a). The peak of spawning takes place in March–May, mainly in the Bay of Biscay and west of Ireland (ICES, 2021a). Afterwards, mackerel migrates farther into the Nordic Seas for feeding during the productive high-latitude summer (Bachiller *et al.*, 2016; Nøttestad *et al.*, 2016). In autumn, mackerel returns to shelf areas off the British Isles and thereafter continues either southwards or to places near the Norwegian Trench to overwinter (Jansen *et al.*, 2012). The following lengthy spawning dynamics of each individual are supported by active feeding
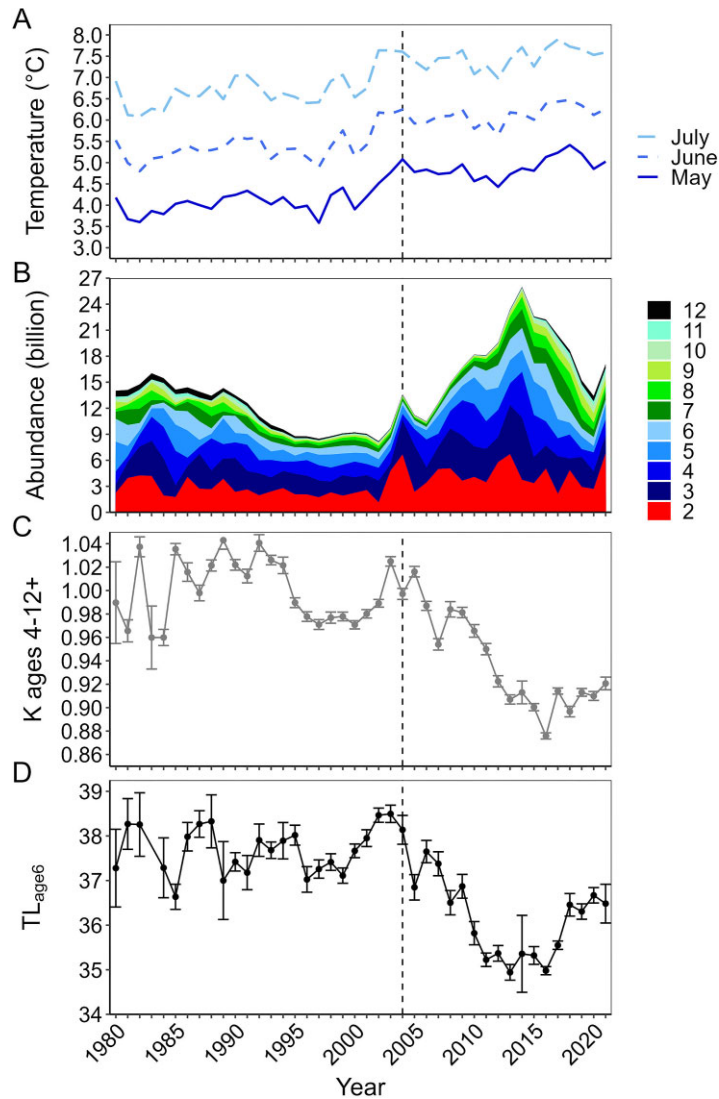
Figure 1. (A) Yearly (1980–2021), modelled mean environmental temperature (0–53 m) in May, June, and July in the proper Norwegian Sea (Supplementary Figure S2), (B) age-specific abundance of mackerel (ages 2 to 12+ years) from 1980 to 2021 (ICES, 2022a), (C) mean and coefficient interval (±95% CI) of body condition (Fulton K = 100 × W/TL³) for sexually mature mackerel (ages 4 to 12+ years), and (D) mean (±95% CI) total length-at-age for 6 years old (TL_age6) mackerel, based on data from the Norwegian purse seine (unselective gear, Slotte *et al.*, 2007) sampled in September and October from 1980 to 2021 (IMR database, see also Olafsdottir *et al.*, 2016; Jansen *et al.*, 2021). Vertical dashed line demarcates the beginning of the current study period (2004–2021).

(Jansen *et al.*, 2021). Thus, mackerel is classified as an income breeder. In terms of reproductive style, mackerel is a multiple (batch) spawner, with an indeterminate fecundity (dos Santos Schmidt *et al.*, 2021; Jansen *et al.*, 2021), spawning pelagically in the upper water column (Coombs *et al.*, 1981). The number of egg batches released is not yet well established but seems to be typically around 20 (dos Santos Schmidt *et al.*, 2021; Jansen *et al.*, 2021). Generally, this reproductive style—in addition to the continued production of developing oocytes during spawning—implies that atresia (oocytes reabsorption) mainly takes place towards the end of spawning (Hunter and Macewicz, 1985; Corriero *et al.*, 2021). However, in the specific case of mackerel, the frequency of atresia increases already from May onwards (dos Santos Schmidt *et al.*, 2021). Atresia is normally triggered by low food intake and/or suboptimal temperatures (Rideout *et al.*, 2005; Corriero *et al.*, 2021).

The dynamics of mackerel distribution appear to be closely linked to a preference for optimal ambient temperatures, though differing between adults and progeny. During the feeding season in the Nordic Seas, mackerel migrates in temperatures ranging from 5 to 15°C but seemingly prefers areas with temperatures between 9 and 13°C (Olafsdottir *et al.*, 2019). The optimal spawning temperature of mackerel, based on experimental egg survival, is around 11°C; the mortality increased significantly at 8°C but also to some degree at higher temperatures, tested up to 18°C (Mendiola *et al.*, 2006). These types of temperature-mediated reproductive responses agree with the results of Bruge *et al.* (2016), who showed that the mean temperature in the mackerel spawning area ranged between 10 and 11°C during 1992–2013. Robert *et al.* (2009) demonstrated that the growth of mackerel larvae in the Gulf of St. Lawrence was tightly linked to the availability of prey but also increased linearly with temperatures from 10 to18°C.

Table 1. The adopted, standardized macroscopic maturity scale, versus the maturity stage scale in use by each of the marine laboratories involved (Supplementary Table S2).

Standardize maturity scale	Norway and Faroe Islands maturity scale[1]	Iceland maturity scale[2]	Denmark and Greenland maturity scale[3]
1–Immature	Immature (a) and Immature (b)	Immature and Juvenile	Immature
2–Early maturing	Maturing (a = early maturing)	Early stage of maturation	Early ripening
3–Mature	Maturing (b = late maturation) and Maturing (c = ripe)	Later stage of gonad maturation and fully mature gonads but not spawning	Late ripening and ripe
4–Spawning and partly spent	Spawning	Spawning and partly spawned	Partially spent
5–Spent and resting	Spent and resting	Has finished spawning and rest stage if previously spawned	Spent and recovery spent

Source: [1]Mjanger *et al*. (2020), [2]ICES (2007), [3]Walsh *et al*. (1990)

These authors argued that reduced availability of preferable prey leads to reduced recruitment through suboptimal feeding and growth, and that the negative impacts on survival at this early trophic bottleneck are amplified when low temperatures prevail during the larval growth season.

Following a warmer ocean (Skagseth and Mork, 2012; Asbjørnsen *et al*., 2019; ICES, 2022b; Skagseth *et al*., 2022), as also reflected in corresponding climate model runs (Figure 1A), and a succession of relatively larger year classes since 2000, the NEA mackerel reached historically high stock levels in 2014 (ICES, 2021b) (Figure 1B). This trajectory likely resulted in stronger intraspecific competition for prey locally, and thereby encouraging distribution expansion both northwards and westwards to new productive feeding areas (Nøttestad *et al*., 2016; Nikolioudakis *et al*., 2019; Olafsdottir *et al*., 2019). Correspondingly, there was a drop in postfeeding (September–October) body condition (Figure 1C) and growth (Figure 1D) to historical low levels (Olafsdottir *et al*., 2016; Jansen *et al*., 2021), which suggests that bioenergetics may have played an important role for the migration choices. It is notable that a significant expansion of the spawning area was observed in the same directions as the main feeding migration during the period when these energetic constraints appeared (Bruge *et al*., 2016; Brunel *et al*., 2018; Chust *et al*., 2023). Hypothetically, mackerel low in energy could be expected to undertake spawning migrations towards increasing prey densities to secure the future rather than current spawning success. This conceptual framework implies that the survival probabilities of their progeny outside the traditional spawning area are traded against the energetic rebuilding of adult body compartments. Such considerations are supported by the fact that eggs and larvae from mackerel spawning far north in the Norwegian Sea would physiologically speaking—according to present knowledge—encounter suboptimal temperatures (Mendiola *et al*., 2006).

Currently, the northern limits of the mackerel spawning area are not yet completely defined. Recent efforts have been made by participating countries during the Triennial Mackerel Egg Survey (ICES, 2021a), showing a northward expansion of spawning areas into the Nordic Seas, in line with Brunel *et al*. (2018) and the most recent study of Chust *et al*. (2023). An exploratory egg survey in June 2021 also showed that mackerel were spawning at latitudes >68°N off the Norwegian coast (ICES, 2021b). The above-mentioned temporal dynamics in ocean warming, stock levels, body growth, and condition

create an ideal backdrop to determine and detail the resulting responses in mackerel spawning distribution changes. The present study concentrated on research survey and commercial fisheries data from the last three months of the spawning season (May–July) with the following objectives: (1) with a basis in macroscopic maturity data, examine to what extent the mackerel spawning activity has been extended into the more traditional feeding areas of the Nordic Seas during the recent (2004–2021) warmer conditions; (2) relate this insight to corresponding information on age, body size, and condition; (3) validate the correctness of the macroscopic staging by a microscopic study on oocyte development; (4) explore if the general ocean warming of the Nordic Seas correspondingly resulted in a larger area with suitable spawning conditions; (5) test if the observed reduction in body growth and postfeeding body condition potentially could be the main reason for extending spawning activities into the Nordic Seas; and (6) based on these aggregated results, discuss any potentially foreseen life-history trade-off between investing into current and future spawning success.

Material and methods
Specimen collections

Mackerel time series datasets (2004–2021) from five countries—Denmark, the Faroe Islands, Greenland, Iceland, and Norway—were collated and used (Supplementary Figure S1 and Table S1). All data refer to the feeding season—from May to July—when mackerel can be found in Nordic waters (Bachiller *et al*., 2016; Nøttestad *et al*., 2016; Nikolioudakis *et al*., 2019; Olafsdottir *et al*., 2019). The southernmost limit of the research area was delineated as latitude 58°N to avoid re-evaluating standard data from the main spawning areas (ICES, 2021a). Hence, all data used, except from the tagging survey (see below), were collected >58°N (Supplementary Figure S1). They originated from the following six collection programmes (Supplementary Figure S1 and Table S1): (i) International Ecosystem Survey of Nordic Seas (IESNS) in May 2008–2021; (ii) data from the Mackerel Tagging Programme of the Institute of Marine Research (IMR) in May 2020–2021, extended northwards of 58°N in these two years only; (iii) mackerel samples from commercial fishing; (iv) opportunistic research surveys from June 2004-2021, except for 2007–2008, (v) Norwegian

research data sets in July (2004–2006, 2008-2009), and (vi) the International Ecosystem Summer Survey of Nordic Seas (IESSNS) in July in 2007 and 2010–2021, which covered both the main feeding area of mackerel in the Norwegian Sea as well as the expansion of feeding migration westwards into Icelandic and Greenland waters (Olafsdottir *et al.*, 2019).

The number of specimens sampled within the area was in total ∼62000 and varied between months and years: highest number in July, ranging from 261 to 5200, and lower in June and May; 0–1189 and 0–477, respectively (Supplementary Table S1). The spatial coverage in the Nordic Seas was also most comprehensive in July, ∼58°–77°N and 42°W–32°E. In June, the sampling was mostly limited to the southern part of the research area, south of 64°N, and along the coast of Norway northwards to 71°N. The sampling in May focused on the central part of the Norwegian Sea, latitude 62–68°N (Supplementary Figure S1 and Table S1).

Specimen measures and macroscopic staging

Each individual was characterized by total length (TL; cm), whole body weight (W; in g), sex, macroscopic maturity stage, and age. Otoliths were used to determinate the age (in years) (Mjanger *et al.*, 2020). Each participating marine laboratory used their own macroscopic maturity scale (Table 1, a detailed description of each maturity scale is presented in Supplementary Table S2). For standardization purposes, a collective maturity scale was established, resulting in a total of five macroscopic maturity stages (Table 1). Only sexually mature individuals (adults) (TL ≥ 28 cm and age ≥ 3 years) (ICES, 2018) were considered. Any incidences of immatures of atypical large size or old age were excluded ($N = 1445$; 2.3% of the original dataset). Relative body condition (K_n) was established between the observed and the predicted body weight, based on the weight-length relationship (Le Cren, 1951): $W_{pred} = 0.0114 \times TL^{2.932}$ ($r^2 = 0.811$, $p < 0.001$).

Ovary processing, microscopic staging, and reproductive measures

A subset of ovaries ($N = 134$) from 2018 underwent histological analysis. These tissue samples were taken randomly across the study area in the months of May (IESNS), June (Post-Larvae Herring Survey), and July (IESSNS) to be preserved in 3.6% buffered formaldehyde. The whole, preserved ovaries were weighed (OW; 0.001 g) back in the laboratory. The histology protocol consisted of dehydrating the tissue in an ascending sequence of ethanol, embedding in historesin (Technovit® 7100), and mounting. The 4-μm-thick slides were stained with toluidine blue and scanned (Hamamatsu S60) at a resolution of 220 nm/pixel (see details in dos Santos Schmidt *et al.*, 2021).

Each female was classified according to the most advanced oocyte phase. A total of 13 oocytes phases were used: previtellogenic oocytes (PVO) 1–3 and 4a–c, cortical alveoli oocytes (CAO), vitellogenic oocytes (VTO) 1–3, germinal vesicle migration (GVM), germinal vesicle breakdown (GVBD), and hydrated oocytes (HYD) (dos Santos Schmidt *et al.*, 2021). For direct comparison with macroscopic stages, all specimens were finally classified as being either spawning capable or spent (see Result Section). Spawning capable referred to females in VTO1 to HYD (based on Heins and Brown-Peterson,

2022), whereas spent to females in PVO4c or CAO (Supplementary Table S3). However, females exhibiting CAO in May 2018 were reclassified as spawning capable when massive atresia (see below) was not an issue. The background for classifying females with CAO in June and July 2018 as spent was that they most likely would not have enough time to complete oogenesis before the spawning season ended (Green-Walker *et al.*, 1994; dos Santos Schmidt *et al.*, 2021) (Supplementary Table S3). Atresia (early-, late-alpha, and beta atresia) and postovulatory follicles (POF) were also identified, as well as any presence of residual egg. A new microscopic-based category was included—"terminating spawning"—which referred to individuals with massive atretic activity (90% of vitellogenic oocytes being atretic [ICES, 2019]), indicating no further possibility to continue spawning in the current season. The gonadosomatic index [GSI (in %); GSI $= 100 \times OW/(W—OW)$] was calculated for all individuals analysed histologically, as well as the associated relative condition (K_n) (as defined earlier).

Ocean temperature simulation

The present temperature hindcast (May, June, and July 1980–2021, 0–53 m depth) consisted of two separate but interlinked approaches: (i) restricted to the Norwegian Sea (Supplementary Figure S2), by adopting the same polygon outline as in Kjesbu *et al.* (2022), to illustrate temperature changes to the main summer feeding area of mackerel, and (ii) broadening the simulation to a significant part of the North Atlantic (latitudes 58°–80°N and meridians ≈15°W and 30°E) to address a possibly extended feeding and suitable spawning area (SSA) westwards and polewards. These graphical maps were followed by calculations of the SSA in km², where the starting value referred to the lowest temperature at which spawning-capable individuals were located during the combined spawning and feeding season (see maturity staging methods above). More specifically, the SSA above a given sea temperature was found by mathematical integration of the geographic area in question, limited to three stepwise increases in this temperature by 1°C, that is, from >8° via >9° to >10°C, but where only the latter temperature is considered optimal for spawning mackerel and egg survival (Mendiola *et al.*, 2006).

The applied NEMO-NAA 10 km is a regional ocean modelling configuration based on the NEMO ocean engine, version 4.0 (Madec and the NEMO system team, 2015), developed at the Institute of Marine Research (Hordoir *et al.*, 2022). As the primary aim of this configuration is to study the evolution of thermohaline processes, this model is run without any kind of restoration on salinity. The atmospheric forcing was based on formulations in Large and Yeager (2009) together with the DFS5.2 data set (Brodeau *et al.*, 2010) up to 1978 (from 1958), and the ERA5 data set (Hersbach *et al.*, 2020) from 1979 onwards, as the ERA5 dataset extends longer into recent years than DFS5.2 (Hordoir *et al.*, 2022). Open boundary conditions were from the GLORYS re-analysis (http://marine.copernicus.eu), which exists from 1993 onwards. For earlier years, a climatology based on the same dataset for the years 1993–2003 was used. Other model details and evaluations with respect to hydrography, large-scale transport, and sea ice extent can be found in Hordoir *et al.* (2022).

Statistics

All statistical analyses were performed using R (version 4.2.0; R Core Team, 2022). Interannual changes in TL-at-age and K_n by maturity stage and month were explored by Generalized Additive Models (GAM; R package mgcv, Wood, 2006). Due to differences in spatial coverage over months, we run a single model for each maturity stage by each month, focusing on spent fish in June and July because of the low number of observations within the other maturity stages at that time. Two different models were thereafter applied, using TL or K_n as response variable. Age was considered both as an explanatory variable but also as a partial effect (by the argument "by") in the smooth function for both location (latitude [Lat] and longitude [Lon]) and years. Sex was included in the model to identify any relevant difference between male and female traits but removed from the fitted model if not significant. All age classes were considered, though the oldest specimens were grouped as 10+ years because of their low abundance. A maximum of five knots in the smoothing function was introduced to avoid overfitting the model. Each model was fitted using a scaled t distribution with an identity link function (Wood $et\ al.$, 2016). The initial models tested for each maturity stage within a month were: TL or K_n = factor (Age_i) + Sex_i + s $(Lon_i, Lat_i,$ by = factor (Age_i), k = 5) + s $(Year_i,$ by = factor (Age_i), k = 5), family = scat (link = "identity"). The best model was selected based on the lowest Akaike Information Criteria (AIC) value, and the model diagnostics indicated no issue with the model (i.e. the dispersion value was around 1 and no residual autocorrelation).

The effect of body condition and growth and environmental parameters on spawning activity were analysed with general linear models, excluding June in this statistical analysis due to the abovementioned opportunistic spatial coverage (Supplementary Figure S1b). Two response variables representing spawning activity >62°N were evaluated (Supplementary Figure S1a and c): the proportion and occurrence of active spawners (mature, spawning, and partly spent, both sexes). The proportion of active spawners was calculated as the total number of active spawners divided by the total number of adult mackerel sampled, whereas the occurrence was calculated as the total number of active spawners divided by the total number of trawl stations with adult mackerel.

In July, a third response variable was modelled—the spawning index—where data from outside the defined core area (62–70°N, 5°W–8°E; Supplementary Figure S3) were also included (Supplementary Figure S1c). The maturity stages were converted into a binary variable, indicating whether an individual was an active spawner (mature, and spawning and partly spent stages combined) or not (early maturing and spent stages). Then, a binomial model was fitted to the data by using GAM with year and latitude as explanatory variable [Spawning index = factor (Year) + s (Lat) + ti (Lat, Year), family = binomial(clogclog)], where ti is the tensor of interaction. Residuals plots (DHARMa package; Hartig, 2022) did not indicate any issue with the model (Supplementary Figure S4). The annual spawning index was derived from the model by predicting the spawning probability from 2004 to 2021 and between 62° and 77°N (divided into 0.1°N intervals). The latitude range was selected to cover the whole extent of the observed mackerel spawning locations, followed by averaging the predicted spawning probability across space for each year.

To explore the environmental influence on the proportion of active spawners, the occurrence of active spawners, and the spawning index, the mean modelled annual (by month) temperature at 0–53 m depth in the Norwegian Sea core area (Figure 1A) and the size of the SSA were added to the respective models. For SSA, the parameter value referred to the estimated area at >8°, >9°, and >10°C, where the last restriction includes the optimal spawning temperature (Mendiola $et\ al.$, 2006). Spawning stock biomass (SSB) (ICES, 2021b) was also considered in the models to address any density-dependent effect. Explanatory variables used to represent body condition and growth were the mean Fulton's condition ($K_{age4-12}$) based on fully mature fish at ages 4–12 years (Figure 1C) and the mean length-at-age 6 (TL_{age6}) (Figure 1D), respectively, both referring to September–October (Olafsdottir $et\ al.$, 2016; Jansen $et\ al.$, 2021). Hence, we linked spawning activity to the level of $K_{age4-12}$ and TL_{age6} from the year prior to spawning because mackerel hardly feeds during overwintering and early spawning migration (from November through March; Jansen $et\ al.$, 2021). Body growth and condition in September and October should thereby mirror the prespawning status. All variables were checked for collinearity (Supplementary Figure S5). We applied a forward selection, that is, each explanatory variable was initially tested, then a new variable was added to the model as long as no collinearity issues were in place. The one found between SSB and $K_{age4-12}$ and TL_{age6} did not affect the model. Then, the best model was selected based on the lowest AIC value.

Results

This study on mackerel (2004–2021) covered the time period when the modelled temperature (0–53 m depth) in the central Norwegian Sea flattened out at a high level, as a result of the more or less continued warming over the last three decades (1980–2021) (Figure 1A). Within each year, the temperature became markedly higher from May to July (Figure 1A).

Macroscopic maturity stages

Over the study period, changes were found in the proportion of the various macroscopic maturity stages (Figure 2A). As no difference was recorded between sexes (two-way ANOVA, $p > 0.05$) (Supplementary Figure S6), male and female data were aggregated (Figure 2A). An overall increase in the proportion of early maturing and mature mackerel (stages 2 and 3) was recorded over the years in May; the presence of these two stages grew from 6.6% in 2008 to 98.8% in 2019 (Figure 2A). In contrast, mackerel sampled in June and July were predominately spent and resting (stage 5), except in June at the beginning and end of the time series, when early maturing and mature individuals were frequently seen, but then at a time when the sampling was limited to the southernmost part of the study area (Figure 2A and Supplementary Table S1). The presence of early maturing, mature, and spawning and partly spent mackerel (stages 2–4) in July increased from 0.77% in 2004 to 17.8% in 2017, but since then staying below 10% (Figure 2A). An exceptional peak in early maturing mackerel was observed in July 2009 (Figure 2A).

In May, most of the mackerel were found between 58° and 66°N (Figure 2B and Supplementary Figure S7). Active spawners were mainly located between 62° and 66°N (Figure 2B).
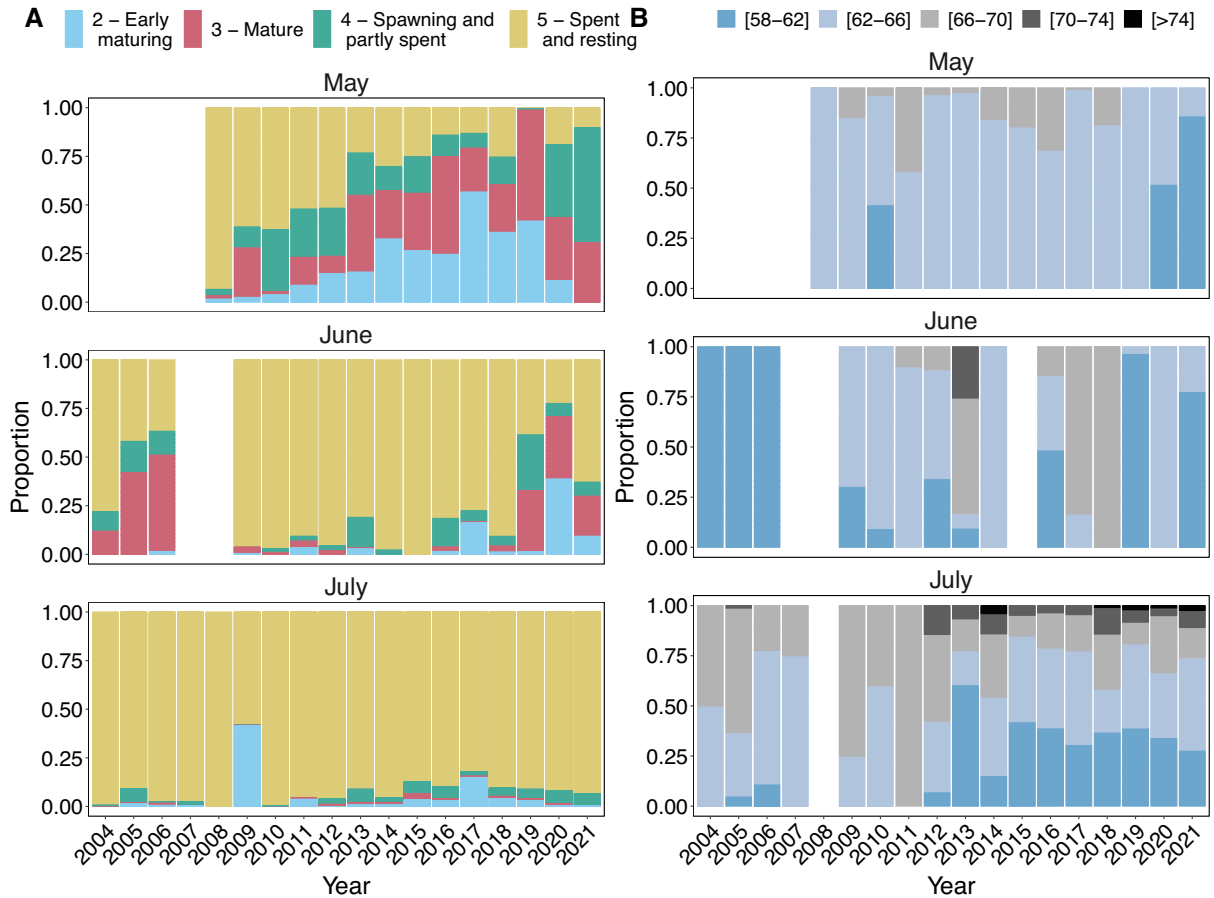
Figure 2. (A) Proportion of each macroscopic maturity stage recorded for mackerel females and males combined, and (B) proportion of active mackerel female and male spawners (macroscopic mature, spawning, and partly spent combined) within five latitude ranges, from May to July 2004–2021.

The high proportion of active spawners recorded <62°N in May 2020–2021 (Figure 2B) mostly referred to data from the tagging survey (Supplementary Figure S4 and Table S1). Females and males often showed extensive spatial overlap (Supplementary Figure S7). Spawning females were recorded east of Iceland in May 2009 and 2010, rather than typically nearer Norway (Supplementary Figure S7). Spawning males were also observed east of Iceland in May 2009. Likewise, spent mackerel were seen in these waters in 2009–2011 (Supplementary Figure S7).

The June samples originated from highly different geographical locations over the years (Figure 2B and Supplementary Figure S8). Early maturing mackerel were detected in 10 out of 16 years (Figure 2A), though collecting only females in 2006, 2016, and 2019, and males in 2009 and 2018 (Supplementary Figure S8). In 2017, the year with the second highest percentage of early maturing mackerel (Figure 2), the majority of the June samples were taken close to the northern Norwegian coast (Lofoten area; ~70°N) (Supplementary Figure S8). The highest percentage of early-maturing mackerel was recorded in 2020 (Figure 2A), close to the Faroe Islands (Supplementary Figure S8). A similar situation was observed the year after, both in terms of geographical location and the reasonably mixed proportion of early-maturing and mature individuals (Figure 2A and Supplementary Figure S8). Active spawners showed a spread distribution over years but were

mostly seen south of 66°N (Figure 2B and Supplementary Figure S8). From 2009 up to 2016, most of these samples referred to locations near Iceland (Supplementary Figure S8). Spawning mackerel were also found close to the Norwegian coast at latitude ~70°N (2012–2013, 2016–2018) (Figure Supplementary S8).

Before 2012, active spawners mackerel collected in July were mainly found at latitudes between 62° and 70°N (Figure 2B), with spawning individuals in southern and central areas, whereas spent individuals in northern (near Jan Mayen) and western areas (near Iceland) (Figure 3). No distribution map could be presented for individuals in early-maturing stages in July due to their low number. A marked change happened from 2012 onwards seeing spawning and partly spent mackerel as far north as 70°N but also examples of such maturity stages even farther north to 74°N (Figures 2B and 3).

Interannual variability in length, age, and body growth

The mean TL of mackerel sampled in May–June showed no clear trend over the study period (Figure 4A), whereas the mean age increased from 4 to 7 years (Figure 4B and Supplementary Figure S9). In May, all maturity stages approximately showed the same type of annual pattern in relation to mean TL and age, though early maturing individuals were generally smaller and younger (Figure 4). In June, mean TL was
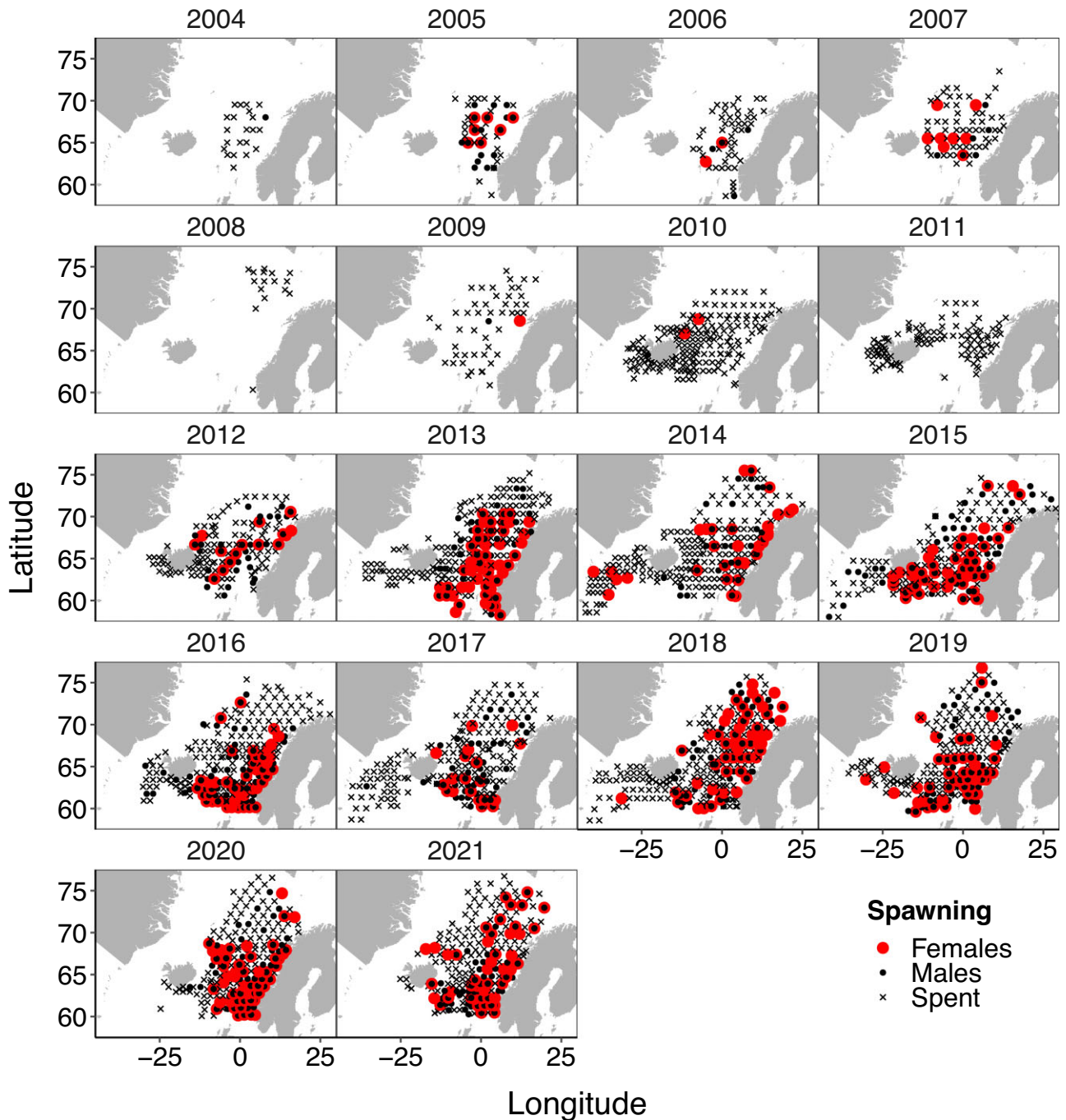
Figure 3. Distribution, based on presence, of macroscopic maturity stages as observed in Nordic waters in July from 2004 to 2021 of spawning and partly spent, and spent mackerel. Females (red circle) and males (black circle) are separately identified as spawning and partly spent but grouped in the spent category (cross symbol).

roughly similar across time, though mean age showed indications of a dome-shaped pattern from 2015 onwards (Figure 4A). In July, the fish size was largest at the beginning and end of the time series (until 2008 and after 2020), and age was highest at the end (Figure 4A and B). Body growth for early-maturing mackerel captured in May aged 5 years and older showed signs of a higher TL-at-age in recent years, but in cases with no clear trend for a given age class (Supplementary Figure S10). However, for spent individuals in June and July , body growth decreased over the study period, resulting in

a smaller difference in TL among age classes (Supplementary Figure S11).

The GAM results on TL-at-age in relation to maturity stage showed a reduction in the percentage of deviance explained in May from 72.7% at the early maturing stage to 59.9% at the spent stage (Table 2, for detailed model outputs see Supplementary Table S4). Sex was a significant factor for spawning (May) and spent fish (June and July) (Table 2, Supplementary Table S4). Geographical position (Lon and Lat) played a significant role for most age classes in May for mature mack-
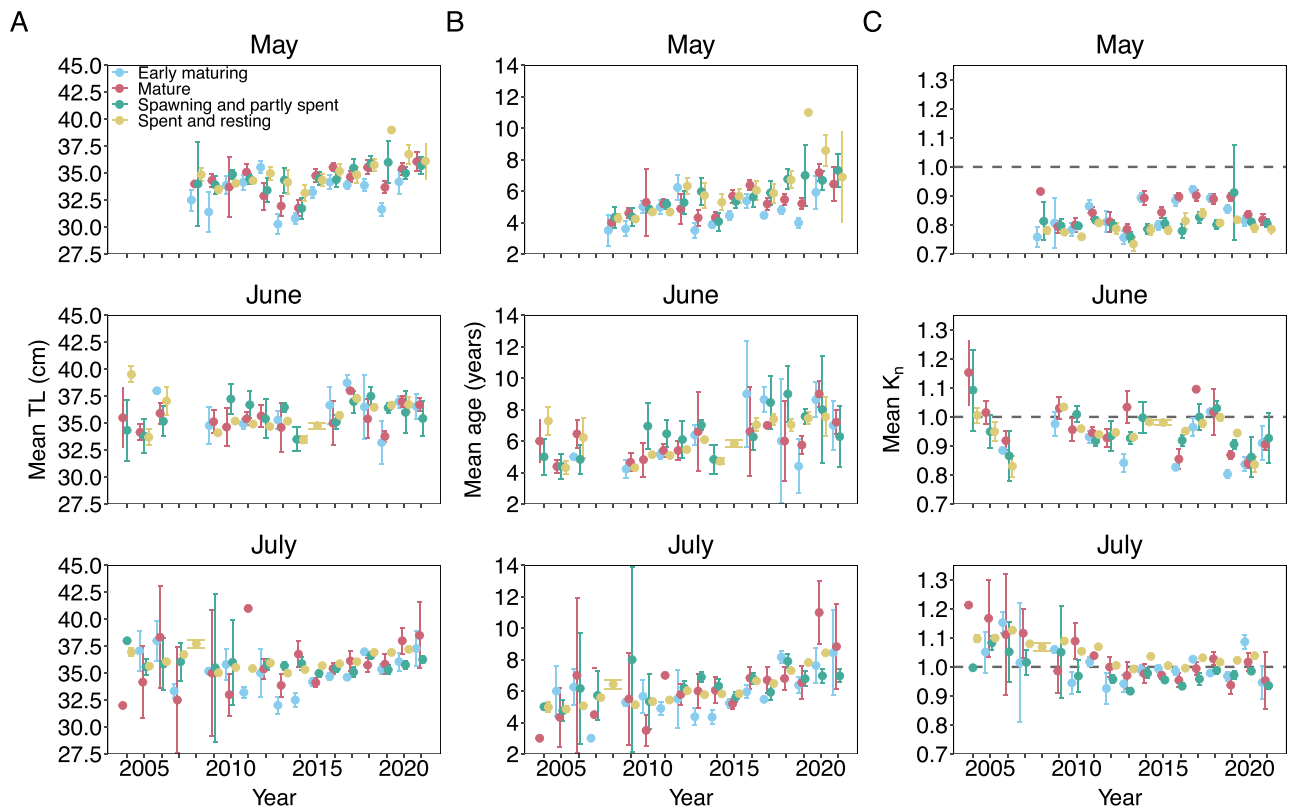
Figure 4. Interannual variation in mean (±95% CI) (A) TL, (B) age, and (C) K_n by macroscopic maturity stage and month (May–July) over years (2004–2021). Horizonal dashed line (C) marks the threshold between good ($K_n \geq 1$) and poor ($K_n < 1$) relative condition.

Table 2. GAM fits comparison among months and maturity stages for both length and relative condition. N is the number of observations in the model, whereas DE is deviance explained. Detailed model output can be found at Supplementary Table S4.

Month	Maturity stage	Response variable	Explanatory variables	N	Adjusted R^2	Total DE (%)
May	Early maturing	Length	Age + s(Lon, Lat, by = age) + s(year, by = age)	901	0.760	72.7
May	Mature	Length	Age + s (Lon, Lat, by = age) + s(year, by = age)	1 005	0.770	72.5
May	Spawning and partly spent	Length	Age + Sex + s (Lon, Lat, by = age) + s(year, by = age)	724	0.727	69.2
May	Spent	Length	Age + s (Lon, Lat, by = age) + s(year, by = age)	1 212	0.671	59.9
June	Spent	Length	Age + Sex + s (Lon, Lat, by = age) + s(year, by = age)	5 515	0.583	58.8
July	Spent	Length	Age + Sex + s(Lon, Lat, by = age) + s(year, by = age)	47 501	0.700	63.9
May	Early maturing	K_n	Sex + s(Lon, Lat, by = age) + s(year, by = age)	901	0.368	34.1
May	Mature	K_n	Age + Sex + s(Lon, Lat, by = age) + s(year, by = age)	1 004	0.263	26.6
May	Spawning and partly spent	K_n	Sex + s(Lon, Lat, by = age) + s(year, by = age)	724	0.116	15.3
May	Spent	K_n	Age + s(Lon, Lat, by = age) + s(year, by = age)	1 212	0.274	26.9
June	Spent	K_n	Age + Sex + s(Lon, Lat, by = age) + s(year, by = age)	5 515	0.100	12.1
July	Spent	K_n	Age + Sex + s(Lon, Lat, by = age) + s(year, by = age)	47 501	0.160	14.7

erel as well as typically "year-by-age" for spent individuals (Supplementary Table S4). In June and July, both location and year were highly influential factors among age classes (Supplementary Table S4). For these two months—restricted to spent individuals—the deviance explained was 58.8 and 63.9%, respectively (Table 2, for detailed model outputs see Supplementary Table S4).

Body condition

Mean K_n increased from May to June, but also to some extent from June to July (Figure 4C). In May, K_n was generally higher for early maturing and mature fish than for spawning and spent fish, but consistently so from 2014 to 2018 (Figure 4C). K_n did not show any clear interannual variation in May and June (Figure 4C). However, K_n in July was consistently lower after 2011. In addition, K_n for 2012–2021 became typically lower for active spawners than those being spent, even if the area investigated was limited to the Norwegian Sea core area (Supplementary Figures S3 and S12). In May, mean K_n-at-age showed a dome-shaped pattern in the end of the time series for early maturing and mature fish, whereas little temporal variation was seen for spawning and spent fish (Supplementary Figure S13). A more dynamic pattern was observed for mean K_n-at-age in June for both of these latter maturity stages; however, in July a minor decrease was recorded from the beginning to the end of the study period (Supplementary Figure S14).

The K_n model explained much less than the TL-at-age model, from 34.1 to 15.3% in May (early maturing-spent), 12.1% in June (spent), and 14.7% in July (spent) (Table 2, for detailed model outputs see Supplementary Table S4). All parameters showed a significant effect on spent fish over the three months (Supplementary Table S4).

Microscopic study

The histological analyses in May, June, and July 2018 detected spawning capable (Figure 5A), terminating spawning (Figures 5B and C), and spent individuals (Figure 5D). Approximately 93% of the studied females in May were spawning capable, but this proportion dropped to <15% in June and July (Figure 6A). Among the relative low proportion of spawning capable females in July about 38% were terminating spawning—that is, absorbing vitellogenic oocytes through atresia (Figure 6A). GSI progressively decreased from spawning capable via terminating spawning to spent mackerel (Figure 6B). Spawning individuals (May–July) were found in the eastern part of the Norwegian Sea, whereas in July terminating spawning and/or spent mackerel were mainly found south of Iceland and in the northern areas of the Norwegian Sea (Figure 6C). Similar to the macroscopic analysis (Figure 4C), the mackerel in May were in relatively poor condition compared to the other two months of study (Supplementary Figure S15). Also, there was an abrupt increase in K_n for spawning females from May to June, though with the three maturity categories levelling off roughly at the same values of K_n in July (Supplementary Figure S15).

Suitable spawning area

Selecting 2018 as an example from this recent, outlined period of ocean warming (Figure 1A), the seasonal (May–July) spread of a warm pulse of water northwards—as represented by the 10°C isotherm, that is, the optimal spawning temperature for mackerel (see Introduction)—was clearly noticeable (Figure 7A). The addition of information on histological staging for the same year indicated that at least females terminating spawning could be detected even at temperatures down to around 8°C (Figures 6C and 7). The existence of this lower threshold for spawning was supported by the 18-year macroscopic data (Figure 3) in combination with the modelled temperature fields (Figure 1A). Including also the SSA at 8°, 9°, and 10°C in the calculation, the size of the SSA markedly enlarged the opposite way, that is, from 10° via 9° to 8°C within a given month (Supplementary Figure S16). In general, SSA exhibited higher values in the present study period of 2004–2021 compared to the two past decades (Figure 7B; Supplementary Figure S16).

Effects on proportion of active spawners and spawning index

Body condition—in comparison with body growth, SSB, ocean temperature, and SSA (in the Norwegian Sea)—was the most important factor explaining the poleward extension of mackerel spawning activities (Table 3; Supplementary Table S5). The use of overwintering condition in the year prior to spawning (September–October) appeared as the main factor in all best-fitted models, showing a high negative effect on the proportion and occurrence of active spawners within defined areas in the Norwegian Sea in both May and July. A similar result was found for the spawning index in July using all data but taking spatial variations in coverage into account (Table 3). These model results indicated that a higher fraction of adults entered the Norwegian Sea to spawn when the overwintering condition is low. As mentioned, body condition was the main factor explaining the northward spawning; however, when adding SSA in the model, there was a slightly improvement in the model fit in most cases (Table 3; Supplementary Table S5). When significant, SSA mostly displayed a negative effect on the extent of northward spawning activities, except for the proportion of active spawners in July (Table 3). Additionally, changes in growth (TL $_{age6}$) significantly ($p = 0.024$) influenced the proportion of active spawners both alone and combined with SSA in various models in May, but this body trait did not exhibit a significant effect on the proportion of active spawners in July or on other response variables in both months (Supplementary Table S5). Mean monthly temperature typically showed a non-significant effect (Supplementary Table S5), whereas SSB played a significant role, however, its addition did not improve the model fits when combined with other variables (Supplementary Table S5).

Discussion

The present study demonstrates that the NEA mackerel stock has extended its spawning activity northwards to 70°N in the Nordic Seas over recent years, and even further polewards to 75°N in some years. Over the last two decades, the North Atlantic Ocean has entered a historic warm period, although with a downward trend after 2016 (Asbjørnsen *et al.*, 2019; Skagseth *et al.*, 2022; ICES, 2022b), as well as the mackerel SSB has doubled (ICES, 2021b), two factors that may have contributed to this expansion of the mackerel spawning area (Brunel *et al.*, 2018). However, our results suggest that the major poleward extension of the mackerel spawning did not happen before 2012, despite of an enlarged area with suitable
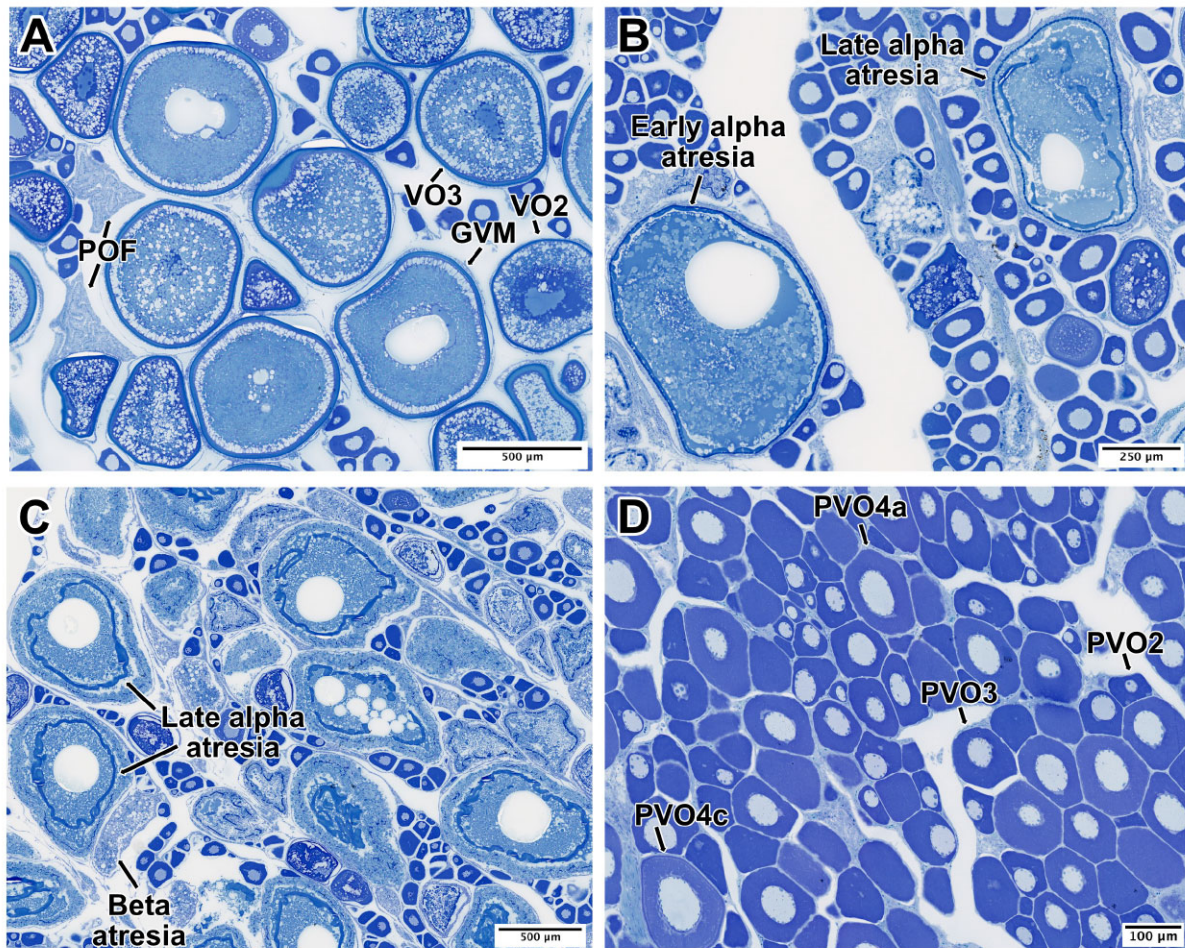
Figure 5. Toluidine blue-stained micrographs of mackerel ovaries in different developmental phases: (A) a spawning capable female, (B and C) females with different degrees of atresia, and (D) a spent female. GVM, germinal vesicle migratory oocyte; POF, postovulatory follicle; PVO, previtellogenic oocyte; VO, vitellogenic oocyte. All images refer to females collected in July 2018.

spawning temperatures being available in the Nordic Seas in May–June since 2002. In fact, the spawning activities here continued at the same level despite the slight decrease in SSA during the month of May in 2004–2021 and a stock decline after 2015. The latter coincides with a decrease of the average heat content trend in the Norwegian Sea after 2016 (Skagseth *et al.*, 2022). Despite so, the major change in spawning distribution corresponded better with the drop in pre-spawning body condition to historical low levels and—to some degree—the reduced size at age (Olafsdottir *et al.*, 2016; Janssen *et al.*, 2021). In addition, the mean size and age of mackerel increased over the study period in correspondence with a decline in recruitment and an ageing stock from the official assessment (ICES, 2022a). Generally, larger, multiple spawners show longer spawning periods (Hixon *et al.*, 2014), increasing the possibility of enhanced offspring survival, cf. the bet-hedging strategy (Hočevar *et al.*, 2021).

Anyhow, it seems unlikely that the extended spawning in space and time so far in July is an adapted strategy to secure increased survival of the progeny, that is, it is more likely to secure better body growth and increased energy for future reproductive processes. We tested the effects of SSA on the poleward spawning based on temperatures at the lower end of observed spawning (>8°C), which would increase egg mor-

tality (Mendiola *et al.*, 2006) and reduce larval growth and survival (Robert *et al.*, 2009), but we also tested for more optimal temperature ranges (>9° and >10°C). Regardless of the chosen temperature range, the trends in SSA over the period 1980–2021 were principally the same, but where the size of the most optimal SSA (>10°C) was considerably smaller than the total area of mackerel observed in > 8°C. More concretely, a most recent exploratory egg survey conducted in June 2021 along the Norwegian coast (from ∼58°N to ∼69°N) detected a low to moderate amount of recently spawned mackerel eggs in waters at 8–9°C (ICES, 2021b). This clarification implies that mackerel can indeed spawn in suboptimal areas for the survival of their progeny but being seemingly optimal in terms of prey availability (Olafsdottir *et al.*, 2019). Regarding the actual fate of mackerel larvae released at these high latitudes, this question is yet open-ended, especially when it comes to those larvae advected into unusually cold-water masses (for mackerel), such as in the Barents Sea and west of Svalbard (Allan *et al.*, 2021). Also, the longer daylight duration comes as another issue (Shoji *et al.*, 2011), possibly heightening predation risk (Allan *et al.*, 2021) but widening the time (search) window for detection of suitable prey (Suthers and Sundby, 1996). In summary, it is doubtful that the progeny of a warm temperate species like mackerel will have higher survival
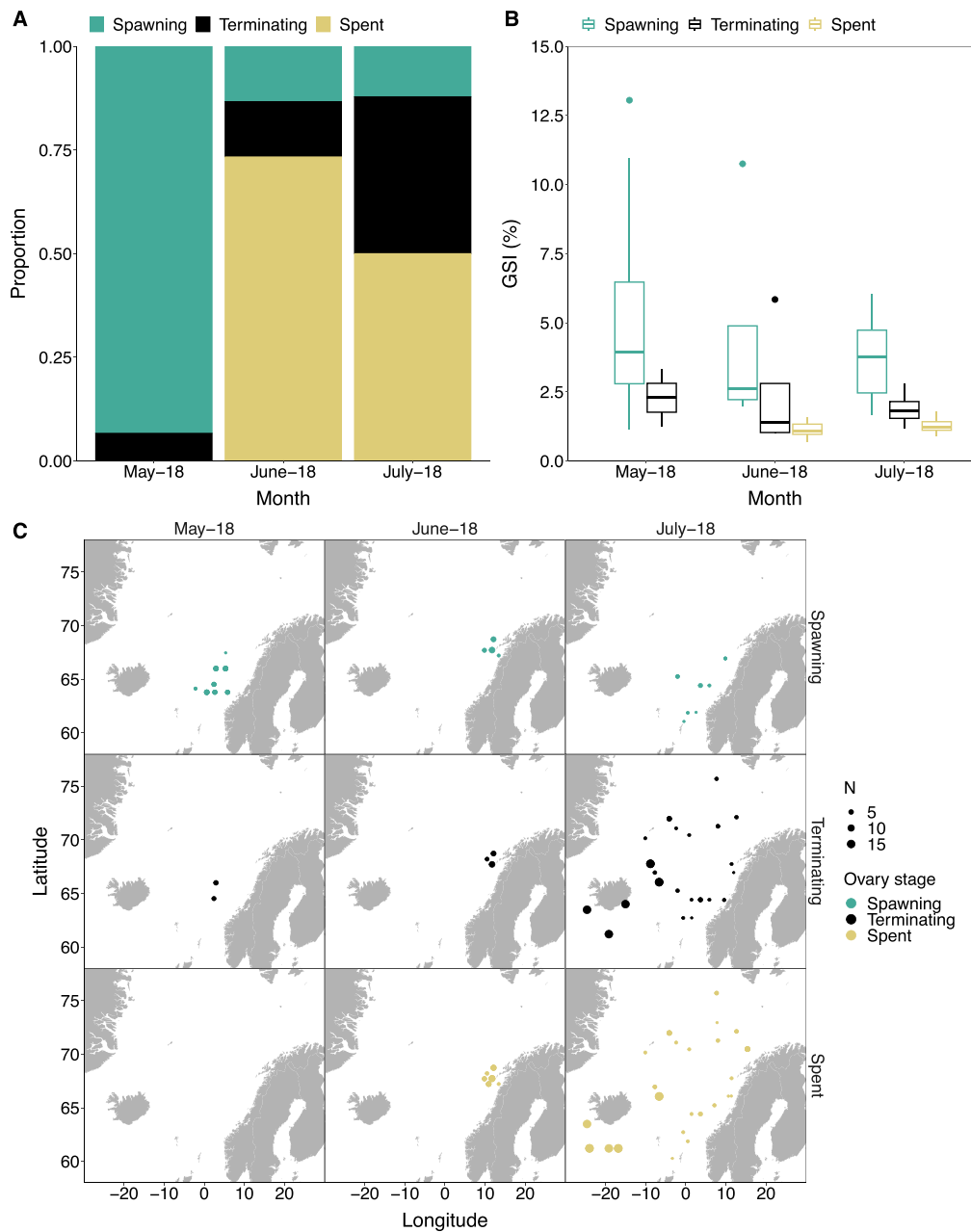
Figure 6. (A) Proportion and (B) GSI by microscopic maturity stage based on subsequent laboratory examination of samples collected in May, June, and July 2018. (C) Spatiotemporal distribution of mackerel females analysed histologically and classified as spawning capable, terminating spawning, and spent. Symbol size in (C) reflects the number of observations.

probabilities in northern waters than more southern waters, where the vast majority spawn (Brunel *et al*., 2018). Finally, a formal distinction should be made between a proximate (underlying) and ultimate (resulting) cause; we consider that an enlarged SSA would refer to the former cause, whereas energetic constrains of the adults to the latter, using then pre-spawning body condition and growth rate as proxies. Hence, our results suggest that the ultimate cause for the poleward spawning activities in recent times is mediated by energetic constraints in a large stock under strict competition for prey.

In view of the multifaceted issue of prey availability, the expansion of the spawning habitat of the conspecific Northwest Atlantic mackerel in the Gulf of Saint Lawrence was significantly better explained when adding zooplankton abun-

dance as an extra explanatory variable to the model (Mbaye *et al*., 2019). Feeding success and thereby better (overwintering) body condition in this stock are closely linked to zooplankton (prey) abundance, composition, and phenology (Plourde *et al*., 2015). Relatedly, Jansen *et al*. (2021) suggested that the NEA mackerel compensates for a low energetic status by feeding during the main spawning season from April onwards. Our results also found a substantial improvement in body condition over the period May–July, when a major part of the stock entered the Norwegian Sea for feeding purposes and the distribution was extended polewards (Nøttestad *et al*., 2016; Nikolioudakis *et al*., 2019; Olafsdottir *et al*., 2019), whilst at the same time the maximum proportions of spawners dropped from about
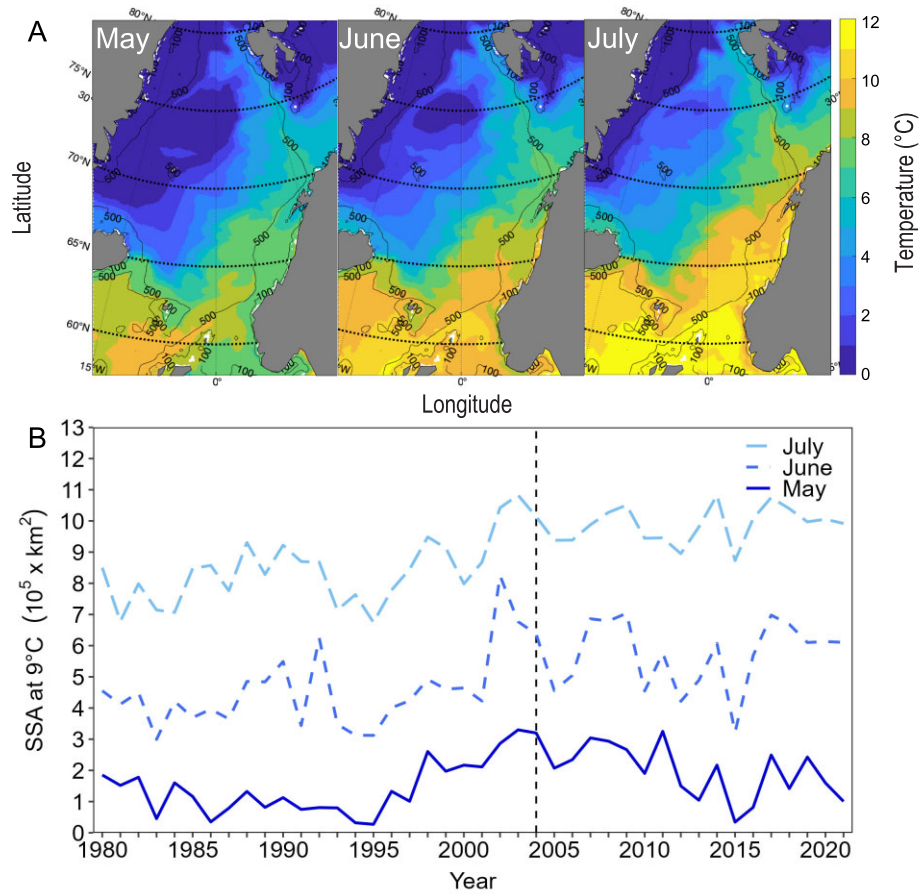
Figure 7. (A) Spatial change in modelled environmental temperature (0–53 m) by 1°C isotherms in the North Atlantic (58°–80°N) in May, June, and July 2018. (B) Suitable spawning area from May to July at 9°C temperature from 1980 to 2021. Vertical dashed line (panel B) demarcates the beginning of the current study period (2004–2021).

Table 3. General linear models result for each fitted model. The best models for each response variable are shown according to AIC criteria, where all explanatory variables were tested (for further details on all models tested, see Supplementary Table S5). Parameter estimated (estimate) and the corresponding standard error (Std. Error) and p-value are given. Mean K represents the mean Fulton's condition at ages 4 to 12 years, whereas SSA refers to the suitable spawning area (see main text).

Month	Response variable	Explanatory variables	Estimate	Std. Error	p-value	Adjusted R^2
May	Proportion of active spawners					0.571
		Intercept	4.367	0.937	<0.001	
		mean $K_{(y-1)}$	-4.186	0.994	<0.001	
		SSA (10°C)	-0.546	0.277	0.068	
May	Occurrence of active spawners					0.460
		Intercept	99.730	23.570	< 0.001	
		mean $K_{(y-1)}$	-97.950	24.910	0.001	
July	Proportion of active spawners					0.526
		Intercept	1.104	4.500	<0.001	
		mean $K_{(y-1)}$	-0.748	-4.287	<0.001	
		SSA (9°C)	0.014	-2.484	0.026	
July	Occurrence of active spawners					0.468
		Intercept	21.117	5.158	0.001	
		mean $K_{(y-1)}$	-14.010	3.670	0.020	
		SSA (9°C)	-0.689	0.290	0.033	
July	Spawning index (62°–77°N)					0.382
		Intercept	0.447	0.121	0.002	
		mean $K_{(y-1)}$	-0.285	0.087	0.005	
		SSA (9°C)	-0.016	0.068	0.376	

75 to 15%. According to diet studies in the Norwegian Sea, mackerel has a high food consumption dominated by the cold-temperate *Calanus finmarchicus* (Langøy *et al.*, 2012; Bachiller *et al.*, 2016). The abundance of this important copepod is tightly linked to plankton blooms propagating northwards in the Atlantic during spring and summer (Friedland *et al.*, 2016), including within the Norwegian Sea (Broms and Melle, 2007), which is the centre of production (Melle *et al.*, 2014). This spatiotemporal pattern of *C. finmarchicus* leaves the mackerel, an income breeder (Jansen *et al.*, 2021), with the option of either terminating spawning farther south from this food source (Brunel *et al.*, 2018) or supporting further gametogenesis by active poleward feeding migration. Our analysis of body condition in July showed a negative temporal trend stabilizing at low levels after 2011 corresponding with observations on pre-spawning fish (Olafsdottir *et al.*, 2016; Janssen *et al.*, 2021) as well as with the noticed poleward extension of spawning. Furthermore, the low proportion of active spawners in July—still having eggs left in the body captivity—were consistently in a poorer condition than those being spent in all years from 2012 to 2021, implying that these late spawners would need to prioritize feeding to rebuild body compartments. These results and considerations support the hypothesis that the major extension of spawning activities late in the season and far polewards in the Norwegian Sea was stimulated by energetic constraints with a trade-off to secure future reproductive success rather than an adaptive strategy to increase the current survival of progeny.

The low condition of NEA mackerel during the stock decline from 2015 onwards suggests that other than pure stock density-dependent effects should be in place; marked changes in the biogeography of *a series* of copepod species in the North Atlantic have been identified under on-going ocean warming (e.g. Beaugrand *et al.*, 2002; Edwards *et al.*, 2020). A reduction in body growth and condition in salmon (*Salmo salar*) over the same period as presently studied for mackerel has been linked to large-scale changes in the ecosystem—referred to as (ecosystem) regime shift—where a decline in the inflow of Arctic water into the Norwegian Sea led to reduced zooplankton production and thereby prey availability (Utne *et al.*, 2021; Utne *et al.*, 2022; Vollseth *et al.*, 2022). A similar result was found for the body growth of Norwegian spring spawning herring (*Clupea harengus*), but this stock managed to increase the body condition to stable high levels by migrating farther west into the Arctic front and extending the feeding season well into late autumn, likely benefiting from zooplankton being able to produce a second generation in a warmer ocean (Homrum *et al.*, 2022). Nevertheless, the summed stock biomass of mackerel, Norwegian spring-spawning herring, and to some extent of blue whiting (*Micromesistius poutassou*)—feeding upon the same zooplankton directly or indirectly (Langøy *et al.*, 2012; Bachiller *et al.*, 2016)—may notably influence the zooplankton levels in the whole Norwegian Sea through top-down processes (Huse *et al.*, 2012). However, model simulations indicate that the gross secondary production *per se* has recently been increasing in this large marine ecosystem as well as along the Norwegian coast (Kjesbu *et al.*, 2022).

Macroscopic staging, GSI data, and/or histology are regularly used within fish biology to determine the reproductive state of a single individual fish, with the first method dominating in field studies when the overall purpose is to back up regular stock advice (Hunter and Macewicz, 1985; Kjesbu *et al.*, 2003). Our protocol comprised all these three methods over the period May–July in 2018, including in the case of histology also annotations of specific oocyte phases (for instance PVO4c), POFs, and atresia (dos Santos Schmidt *et al.*, 2021). This microscopic examination verified that the corresponding macroscopic data resulted in very much the same type of insights regarding the mackerel's seasonal and spatial reproductive patterns, yet clarifying that 38% of the low proportion of spawning capable females in July terminated their spawning by atresia. Atresia activity normally increases towards the end of the spawning season (Greer-Walker *et al.*, 1994), especially in indeterminate spawners, such as mackerel (dos Santos Schmidt *et al.*, 2021; Jansen *et al.*, 2021). The process of termination of spawning can therefore be reasonably well defined based on the frequency of females with high levels of alpha atresia (Hunter and Macewicz, 1985). In mackerel, the duration (turnover rate) of early atresia stages seems to be around 9 d (Witthames and Greer-Walker, 1991), though expected to vary considerably with ambient temperature (Kurita *et al.*, 2003). Abrupt changes in encountered temperature may also induce atresia in itself (Rideout *et al.*, 2000; Corriero *et al.*, 2021). The waters around Iceland are particularly interesting in this respect: the warm Irminger Current approaches Iceland from the southeast but with the cold East Icelandic Current in close vicinity, creating sharp, local temperature clines (Vilhjálmsson, 2002; Nøttestad *et al.*, 2021). As mackerel is an active swimmer but also an opportunistic feeder (Langøy *et al.*, 2012; Bachiller *et al.*, 2016; Nøttestad *et al.*, 2016), moving into cold water masses enriched with zooplankton (Bachiller *et al.*, 2016) may induce atresia, which could explain the relatively high presence of mackerel terminating spawning in this particular subarea in July. Additionally, the observed reabsorption of oocytic material far polewards in the Norwegian Sea feeding area in July follows the general life history principle of a trade-off between current and future reproductive processes: our interpretation is that mackerel simply end spawning to put efforts into feeding migration to gain enough energy for later physiological/reproductive demands (Olafsdottir *et al.*, 2016; Jansen *et al.*, 2021).

It should be emphasized that our study is based on dynamics in the later part of the spawning season, that is, on relatively small proportions of the total stock extending their spawning towards the north-western edges of the total distribution not being covered by the international triannual egg surveys. Brunel *et al.* (2018) investigated potential factors explaining the overall changes in mackerel spawning distribution based on these egg survey data but did not find any evidence for environmental effects. Contrarily, Chust *et al.* (2023) reasoned that the poleward shift in egg distribution was linked to ocean warming. These patterns of poleward shifts may come with a corresponding contraction in the south: distribution model simulations under different climate change scenarios indicate that the spawning area for NEA mackerel off the Iberian Peninsula will be mostly negatively affected, whilst those west of Ireland and Scotland will suffer less (Fernandes *et al.*, 2020). Moreover, a northward expansion of this species is also seen on the other side of the North Atlantic, where the Atlantic Bight is expected to become a less suitable larval habitat for Northwest Atlantic mackerel, implying that coastal regions farther north, the Gulf of Maine and Gulf of Saint Lawrence, will seemingly favour spawning and recruitment success (McManus *et al.*, 2017; Mbaye *et al.*, 2019).

Conclusions

This investigation shows that the spawning area of NEA mackerel has been significantly extended polewards over the last decade, detecting spawning females and males as far north as 70°–75°N. One limitation in our data sets is the difference in coverage area between years and months, though this issue should be of minor importance in July, that is, in the month with the most far-reaching geographical position of the expanding edge of spawning activity. The macroscopic data seem reliable to their specific purpose, as confirmed by the microscopic analysis. Although so, the level of atresia cannot be properly assessed by the macroscopic investigation alone. The well-developed existence of this cellular process in terminating spawning females strengthens our hypothesis that the outlined behaviour of mackerel is likely not an adaptive strategy to secure increased survival of the progeny but rather a trade-off to secure future reproductive success in a period with high competition for prey. There are five main reasons behind our conclusion: (1) the timing of the major extension of spawning into the Nordic Seas was delayed about 10 years according to when the area had optimal spawning temperatures ($\geq \sim 10°C$), (2) over the study period more fish spawned in the Norwegian Sea at the same time as the size of the area with optimal spawning temperatures was showing signs of decreasing, (3) these spawning activities continued even after 2015 when the stock declined, (4) the timing of poleward spawning fits well with the drop in body growth and condition to the lowest level within the time series, and (5) mackerel—when searching for prey—also spawned in areas with temperatures considered suboptimal for egg and larval survival ($\geq 8°C$), therefore, it seems unlikely that the progeny will survive better that far north than in the traditional spawning areas farther south. A question that remains for future studies is if the energetic constraints due to slower body growth and reduced condition in the stock also may explain some of the *overall* shift in egg distributions, given the extensive migration distances from the wintering areas along Shetland to the Spanish coast, which occur early in the year when prey availability is sparse.

Acknowledgements

Supplementary data

Supplementary material is available at the *ICESJMS* online version of the manuscript.

Funding

Data availability statement

Survey data on mackerel are available from the PGNAPES data base hosted by the Faroe Marine Research Institute.

Conflict of interest

The authors declare that they have no known competing financial interests or personal relationships that could have appeared to influence the work reported in this paper.

References

Alix, M., Kjesbu, O.S., and Anderson, K.C. 2020. From gametogenesis to spawning: how climate-driven warming affects teleost reproductive biology. Journal of Fish Biology, 97: 607–632.

Allan, B.J.M., Ray, J.L., Tiedemann, M., Komyakova, V., Vikebø, F., Skaar, K.S., Stiasny, M.H. *et al.* 2021. Quantitative molecular detection of larval Atlantic herring (*Clupea harengus*) in stomach contents of Atlantic mackerel (*Scomber scombrus*) marks regions of predation pressure. Scientific Reports, 11: 5095.

Asbjørnsen, H., Årthun, M., Skagseth, Ø., and Eldevik, T. 2019. Mechanisms of ocean heat anomalies in the Norwegian Sea. Journal of Geophysical Research: Oceans, 124: 2908–2923.

Astthorsson, O.S., Valdimarsson, H., Gudmundsdottir, A., and Óskarsson, G.J. 2012. Climate-related variations in the occurrence and distribution of mackerel (*Scomber scombrus*) in Icelandic waters. ICES Journal of Marine Science, 69: 1289–1297.

Bachiller, E., Skaret, G., Nøttestad, L., and Slotte, A. 2016. Feeding ecology of Northeast Atlantic mackerel, Norwegian spring-spawning herring and blue whiting in the Norwegian Sea. PLoS ONE, 11: e0149238.

Baudron, A.R., Brunel, T., Blanchet, M.A., Hidalgo, M., Chust, G., Brown, E.J., Kleisner, K.M. *et al.* 2020. Changing fish distributions challenge the effective management of European fisheries. Ecography, 43: 494–505.

Beaugrand, G., Reid, P.C., Ibañez, F., Lindley, J.A., and Edwards., M. 2002. Reorganization of North Atlantic marine copepod biodiversity and climate. Science 296: 1692.

Berge, J., Heggland, K., Lønne, O.J., Cottier, F., Hop, H., Gabrielsen, G.W., Nøttestad, L. *et al.* 2015. First records of Atlantic mackerel (*Scomber scombrus*) from the Svalbard Archipelago, Norway, with possible explanations for the extension of its distribution. Arctic, 68: 54.

Boyd, R., Thorpe, R., Hyder, K., Roy, S., Walker, N., and Sibly, R. 2020. Potential consequences of climate and management scenarios for the Northeast Atlantic mackerel fishery. Frontiers in Marine Science, 7: 639.

Brodeau, L., Barnier, B., Treguier, A.-M., Penduff, T., and Gulev, S. 2010. An ERA40-based atmospheric forcing for global ocean circulation models. Ocean Modelling, 31: 88–104.

Broms, C., and Melle, W. 2007. Seasonal development of *Calanus finmarchicus* in relation to phytoplankton bloom dynamics in the Norwegian Sea. Deep Sea Research Part II: Topical Studies in Oceanography, 54: 2760–2775.

Bruge, A., Alvarez, P., Fontán, A., Cotano, U., and Chust, G. 2016. Thermal niche tracking and future distribution of Atlantic mackerel spawning in response to ocean warming. Frontiers in Marine Science, 3: 86.

Brunel, T., van Damme, C.J.G., Samson, M., and Dickey-Collas, M. 2018. Quantifying the influence of geography and environment on the northeast Atlantic mackerel spawning distribution. Fisheries Oceanography, 27: 159–173.

Cheung, W.W.L., Lam, V.W.Y., Sarmiento, J.L., Kearney, K., Watson, R., and Pauly, D. 2009. Projecting global marine biodiversity impacts under climate change scenarios. Fish and Fisheries, 10: 235–251.

Chust, G., Taboada, F.G., Alvarez, P., and Ibaibarriaga, L. 2023. Species acclimatization pathways: latitudinal shifts and timing adjustments to track ocean warming. Ecological indicators, 146: 109752.

Coombs, S.H., Pipe, R.K., and Mitchell, C.E. 1981. The vertical distribution of eggs and larvae of blue whiting (*Micromesistius poutassou*) and mackerel (*Scomber scombrus*) in the eastern North Atlantic and North Sea. Rapports et Procès-Verbaux des Réunions du Conseil International pour l'Exploration de la Mer, 178: 188–195.

Corriero, A., Zupa, R., Mylonas, C.C., and Passatino, L. 2021. Atresia of ovarian follicles in fishes, and implications and uses in aquaculture and fisheries. Journal of Fish Diseases, 44: 1271–1291.

Cunningham, C.L., Reid, D.G., McAllister, M.K., Kirkwood, G.P., and Darby, C.D. 2007. A Bayesian state-space model for mixed-stock migrations, with application to Northeast Atlantic mackerel *Scomber scombrus*. African Journal of Marine Science, 29: 347–367.

dos Santos Schmidt, T.C., Thorsen, A., Slotte, A., Nøttestad, L., and Kjesbu, O.S. 2021. First thorough assessment of *de novo* oocyte recruitment in a teleost serial spawner, the Northeast Atlantic mackerel (*Scomber scombrus*) case. Scientific Reports, 11: 21795.

Edwards, M., Atkinson, A., Bresnan, E., Helaouet, P., McQuatters-Gollup, A., Ostle, C., Pitois, S. *et al.* 2020. Plankton, jellyfish and climate in the North-East Atlantic. MCCIP Science Review, 2020: 322–353.

Fernandes, J.A., Frölicher, T.L., Rutterford, L.A., Erauskin-Extramiana, M., and Cheung, W.W.L. 2020. Changes of potential catches for North-East Atlantic small pelagic fisheries under climate change scenarios. Regional Environmental Change, 20: 116.

Fogarty, H.E., Burrows, M.T., Pecl, G.T., Robinson, L.M., and Poloczanska, E.S. 2017. Are fish outside their usual ranges early indicators of climate-driven range shifts? Global Change Biology, 23: 2047–2057.

Friedland, K.D., Record, N.R., Asch, R.G., Kristiansen, T., Saba, V.S., Drinkwater, K.F., Henson, S. *et al.* 2016. Seasonal phytoplankton blooms in the north Atlantic linked to the overwintering strategies of copepods. Elementa, 2016: 1–19.

Greer-Walker, M., Witthames, P.R., and Bautista de los Santos, I. 1994. Is the fecundity of the Atlantic mackerel (*Scomber scombrus*: Scombridae) determinate? Sarsia, 79: 13–26.

Hartig, F. 2022. _DHARMa: residual diagnostics for hierarchical (multi-level/mixed) regression models_. R package version 0.4.6, https://CRAN.R-project.org/package=DHARMa (last access 01 May 2023).

Heins, D.C., and Brown-Peterson, N.J. 2022.The reproductive biology of small fishes and the clutch concept: combining macroscopic and histological approaches. Aquaculture, Fish and Fisheries, 2: 253–264.

Hersbach, H., Bell, B., Berrisford, P., Hirahara, S., Horányi, A., Muñoz-Sabater, J., Nicolas, J. *et al.* 2020. The ERA5 global reanalysis. Quarterly Journal of the Royal Meteorological Society, 146: 1999–2049.

Hixon, M.A., Johnson, D.W., and Sogard, S.M. 2014. BOFFFFs: on the importance of conserving old-growth age structure in fishery populations. ICES Journal of Marine Science, 71: 2171–2185.

Hočevar, S., Hutchings, J.A., and Kuparinen, A. 2021. Multiple-batch spawning as a bet-hedging strategy in highly stochastic environments: an exploratory analysis of Atlantic cod. Evolutionary Applications, 14: 1980–1992.

Homrum, E.í., Óskarsson, G.J., Ono, K., Hølleland, S., and Slotte, A. 2022. Changes towards stable good somatic condition and increased gonad investment of Norwegian spring-spawning herring (*Clupea harengus*) after 2005 are linked to extended feeding period. Frontiers in Marine Science, 9: 803171.

Hordoir, R., Skagseth, Ø., Ingvaldsen, R.B., Sandø, A.B., Löptien, U., Dietze, H., Gierisch, A. M. U *et al.* 2022. Changes in arctic stratification and mixed layer depth cycle. Journal of Geophysical Research: Oceans, 127: e2021JC017270.

Hunter, J.R., and Macewicz, B.J. 1985. Rates of atresia in the ovary of captive and wild Northern anchovy, *Engraulis mordax*. Fishery Bulletin, 28: 119–136.

Huse, G., Holst, J.C., Utne, K., Nøttestad, L., Melle, W., Slotte, A, Ottersen, G. *et al.* 2012. Effects of interactions between fish populations on ecosystem dynamics in the Norwegian Sea—results of the INFERNO project. Marine Biology Research, 8: 415–419.

ICES. 2007. Report of the workshop on sexual maturity staging of mackerel and horse mackerel (WKMSMAC) 6–29 November 2007, Lisbon, Portugal. ICES CM 2007/ACFM:26. p.52. https://doi.org/10.17895/ices.pub.19268321

ICES. 2018. Report of the workshop on mackerel biological parameter quality indicators (WKMACQI), 15–17 May 2018, IJmuiden, The Netherlands. ICES CM 2018/EOSG 34. p.42. https://doi.org/10.17895/ices.pub.8177

ICES. 2019. Manual for the AEPM and DEPM estimation of fecundity in mackerel and horse mackerel (WGMEGS), Version 12. Series of ICES Survey Protocols. p.84. https://doi.org/10.17895/ices.pub/5139

ICES. 2021a. ICES working group on mackerel and horse mackerel egg surveys (WGMEGS: outputs from 2020 meeting) ICES Scientific Reports. 3:11. p.88. https://doi.org/10.17895/ices.pub.7899

ICES. 2021b. ICES working group on widely distributed stocks (WGWIDE). ICES Scientific Reports. 3:95. p.874. http://doi.org/10.17895/ices.pub.8298

ICES. 2022a. ICES working group on widely distributed stocks (WGWIDE). ICES Scientific Reports. 4:73. p.922. http://doi.org/10.17895/ices.pub.21088804

ICES. 2022b. Norwegian Sea ecoregion—ecosystem overview.Report of the ICES Advisory Committee, 2022. ICES Advice 2022, Section 12.1. https://doi.org/10.17895/ices.advice.21731726

Jansen, T., Campbell, A., Kelly, C., Hátún, H., and Payne, M.R. 2012. Migration and fisheries of North East Atlantic mackerel (*Scomber scombrus*) in autumn and winter. PLoS ONE, 7: e51541.

Jansen, T., Campbell, A., Brunel, T., and Clausen, L.W. 2013. Spatial segregation within the spawning migration of North Eastern Atlantic mackerel (*Scomber scombrus*) as indicated by juvenile growth patterns. PLoS ONE, 8: e58114.

Jansen, T., Slotte, A., dos Santos Schmidt, T.C., Sparrevohn, C.R., Jacobsen, J.A., and Kjesbu, O.S. 2021. Bioenergetics of egg production in Northeast Atlantic mackerel changes the perception of fecundity type and annual trends in spawning stock biomass. Progress in Oceanography, 198: 102658.

Kjesbu, O.S., Hunter, J.R., and Witthames, P.R. (Eds.). 2003. Modern approaches to assess maturity and fecundity of warm- and cold-water fish and squids. 12, p. 140.

Kjesbu, O.S., Bogstad, B., Devine, J.A., Gjøsæter, H., Howell, D., Ingvaldsen, R.B., Nash, R.D. *et al.* 2014. Synergies between climate and management for Atlantic cod fisheries at high latitudes. Proceedings of the National Academy of Sciences, 111: 3478–3483.

Kjesbu, O.S., Sundby, S., Sandø, A.B., Alix, M., Hjøllo, S.S., Tiedemann, M., Skern-Mauritzen, M. *et al.* 2022. Highly mixed impacts of near-future climate change on stock productivity proxies in the North East Atlantic. Fish and Fisheries, 23: 601–615.

Kurita, Y., Meier, S., and Kjesbu, O.S. 2003. Oocyte growth and fecundity regulation by atresia of Atlantic herring (*Clupea harengus*) in relation to body condition throughout the maturation cycle. Journal of Sea Research, 49: 203–219.

Langøy, H., Nottestad, L., Skaret, G., Broms, C., and Fernö, A. 2012. Overlap in distribution and diets of Atlantic mackerel (*Scomber scombrus*), Norwegian spring-spawning herring (*Clupea harengus*) and blue whiting (*Micromesistius poutassou*) in the Norwegian Sea during late summer. Marine Biology Research, 8: 442–460.

Large, W.G., and Yeager, S.G. 2009. The global climatology of an interannually varying air-sea flux data set. Climate Dynamics, 33: 341–364.

Le Cren, E.D. 1951. The length-weight relationship and seasonal cycle in gonad weight and condition in the perch (*Perca fluviatilis*). The Journal of Animal Ecology, 20: 201–219.

Madec, G., and The NEMO system team. 2015. Nemo ocean engine, version 3.6 stable. Report. http://www.nemo-ocean.eu/Morison last access 2 May 2023.

Mbaye, B., Doniol-Valcroze, T., Brosset, P., Castonguay, M., van Beveren, E., Smith, A., Lehoux, C. *et al.* 2020. Modelling Atlantic mackerel spawning habitat suitability and its future distribution in the north-west Atlantic. Fisheries Oceanography, 29: 84–99.

McManus, M.C., Hare, J.A., Richardson, D.E., and Collie, J.S. 2018. Tracking shifts in Atlantic mackerel (*Scomber scombrus*) larval habitat suitability on the northeast U.S. Continentla Shelf. Fisheries Oceanography, 27: 49–62.

Melle, W., Runge, J.A., Head, E., Plourde, S., Castellani, C., Licandro, P., Pierson, J *et al.* 2014. The North Atlantic Ocean as habitat for *Calanus finmarchicus*: environmental factors and life history traits. Progress in Oceanography, 129: 244–284.

Mendiola, D., Alvarez, P., Cotano, U., Etxebeste, E., and de Murguia, A.M. 2006. Effects of temperature on development and mortality of Atlantic mackerel fish eggs. Fisheries Research, 80: 158–168.

Mjanger, H., Svendsen, B.V., Senneset, H., Fuglebakk, E., Skage, M.L., Diaz, J., Johansen, G.O. *et al.* 2020. Handbook for Sampling Fish, Crustaceans and Other Invertebrates. p. 146. Institute of Marine Research, Bergen.

Nikolioudakis, N., Skaug, H.J., Olafsdottir, A.H., Jansen, T., Jacobsen, J.A., and Enberg, K., 2019. ICES Journal of Marine Science, 76: 530–548.

Nøttestad, L., Utne, K., Óskarsson, G., Jonsson, S., Jacobsen, J.A., Tangen, Ø., Anthonypillai, V. *et al.* 2016. Quantifying changes in abundance, biomass and spatial distribution of Northeast Atlantic (NEA) mackerel (*Scomber scombrus*) in the Nordic Seas from 2007 to 2014. ICES Journal of Marine Science, 73: 359–373.

Nøttestad, L., Anthonypillai, V., dos Santos Schmidt, T.C., Olafsdottir, A.H., Kennedy, J., Jacobsen, J.A., Smith, A.D. *et al.* 2021. Cruise report from the International Ecosystem Summer Survey in the Nordic Seas (IESSNS) 30th June–3rd August 2021. ICES Working Group on Widely Distributed Stocks (WGWIDE, No. 09) ICES HQ, Copenhagen, Denmark, (digital meeting) 25. – 31. August 2021. p.60.

Olafsdottir, A.H., Slotte, A., Jacobsen, J.A., Óskarsson, G.J., Utne, K.R., and Nøttestad, L. 2016. Changes in weight-at-length and size-at-age of mature Northeast Atlantic mackerel (*Scomber scombrus*) from 1984 to 2013: effects of mackerel stock size and herring (*Clupea harengus*) stock size. ICES Journal of Marine Science, 73: 1255–1265.

Olafsdottir, A.H., Utne, K.R., Jacobsen, J.A., Jansen, T., Óskarsson, G.J., Nøttestad, L., Elvarsson, B. Þ. *et al.* 2019. Geographical expansion of Northeast Atlantic mackerel (*Scomber scombrus*) in the Nordic Seas from 2007 to 2016 was primarily driven by stock size and constrained by low temperatures. Deep Sea Research Part II: Topical Studies in Oceanography, 159: 152–168.

Plourde, S., Grégoire, F., Lehoux, C., Galbraith, P.S., Castonguay, M., and Ringuette, M. 2015. Effect of enviromnetal variability on body condition and recruitment success of Atlantic mackerel (*Scomber scombrus* L.) in the Gulf of St. Lawrence. Fisheries Oceanography, 24: 347–363.

Poloczanska, E.S., Burrows, M.T., Brown, C.J., García Molinos, J., Halpern, B.S., Hoegh-Guldberg, O., Kappel, C.V. *et al.* 2016. Responses of marine organisms to climate change across oceans. Frontiers in Marine Science, 3: 62.

Pörtner, H.O., and Peck, M.A. 2010. Climate change effects on fishes and fisheries: towards a cause-and-effect understanding. Journal of Fish Biology, 77: 1745–1779.

R Core team. 2022. R: a language and environment for statistical computing version 4.2.0. https://www.R-project.org/ (last access 21 May 2023).

Rideout, R.M., Burton, M.P.M., and Rose, G.A. 2000. Observations on mass atresia and skipped spawning in northern Atlantic cod, from Smith Sound, Newfoundland. Journal of Fish Biology, 57: 1429–1440.

Rideout, R.M., Rose, G.A.,and and Burton, M. P. M. 2005. Skipped spawning in female iteroparous fishes. Fish and Fisheries, 6: 50–72.

Robert, D., Castonguay, M., and Fortier, L. 2009. Effects of preferred prey density and temperature on feeding success and recent growth in larval mackerel of the southern Gulf of St. Lawrence. Marine Ecology Progress Series. 377: 227–237.

Sandø, A.B., Johansen, G.O., Aglen, A., Stiansen, J.E., and Renner, A. H. H. 2020. Climate change and new potential spawning sites for Northeast Arctic cod. Frontiers in Marine Science, 7: 28.

Shoji, J., Toshit, S.-I., Mizuno, K.-I., Kamimura, Y., Hori, M., and Hirakawa, K. 2011. Possible effects of global warming on fish recruitment: shifts in spawning season and latitudinal distribution can alter growth of fish early stages through changes in daylength. ICES Journal of Marine Science, 68: 1165–1169.

Skagseth, Ø., and Mork, K.A. 2012. Heat content in the Norwegian Sea, 1995–2010. ICES Journal of Marine Science, 69: 826–832.

Skagseth, Ø., Broms, C., Gundersen, K., Hátún, H., Kristiansen, I., Larsen, K.M.H., Mork, K.A. *et al.* 2022. Arctic and Atlantic waters in the Norwegian Basin, between year variability and potential ecosystem implications. Frontiers in Marine Science, 9: 831739.

Slotte, A., Skagen, D., and Iversen, S.A.2007. Size of mackerel in research vessel trawls and commercial purse-seine catches: implications for acoustic estimation of biomass. ICES Journal of Marine Science, 64: 989–994.

Sundby, S., Drinkwater, K.F., and Kjesbu, O.S. 2016. The North Atlantic Spring-Bloom System–Where the changing climate meets the winter dark. Frontiers in Marine Science, 3: 28.

Suthers, I.M., and Sundby, S. 1996. Role of the midnight sun: comparative growth of pelagic juvenile cod (*Gadus morhua*) from the Arcto-Norwegian and a Nova Scotian stock. ICES Journal of Marine Science, 53: 827–836.

Trenkel, V.M., Huse, G., MacKenzie, B.R., Alvarez, P., Arrizabalaga, H., Castonguay, M., Goñi, N. *et al.* 2014. Comparative ecology of widely distributed pelagic fish species in the North Atlantic: implications for modelling climate and fisheries impacts. Progress in Oceanography, 129: 219–243.

Utne, K.R., Pauli, B.D., Haugland, M., Jacobsen, J.A., Maoileidigh, N., Melle, W., Broms, C.T. *et al.* 2021. Poor feeding opportunities and reduced condition factor for salmon post-smolts in the Northeast Atlantic Ocean. ICES Journal of Marine Science, 78: 2844–2857.

Utne, K., Skagseth, O., Wennevik, V., Broms, C.T., Melle, W., and Thorstad, E.B. 2022. Impacts of a changing ecosystem on the feeding and feeding conditions for Atlantic salmon during the first months at sea. Frontiers in Marine Science 9:824614.

Vilhjálmsson, H. 2002. Capelin (*Mallotus villosus*) in the Iceland-East Greenland-Jan Mayen ecosystem. ICES Journal of Marine Science, 59: 870–883.

Vollset, K.W., Urdal, K., Utne, K., Thorstad, E.B., Sægrov, H., Raunsgard, A., Skagseth, Ø. *et al.* 2022. Ecological regime shift in the Northeast Atlantic revealed from the unprecedented reduction in marine growth of Atlantic salmon. Science Advances, 8: eabk2542.

Walsh, M., Hopkins, P., Witthames, P.R., Greer-Walker, M., and Watson, J. 1990. Estimation of total potential fecundity and atresia in the western mackerel stock, 1989. ICES CM Documents, H, 31: 1–22.

Wang, J.-Y., Kuo, T.-C., and Hsieh, C.-H. 2020. Causal effects of population dynamics and environmental changes on spatial variability of marine fishes. Nature Communications, 11: 2635.

Witthames, P.R., and Greer-Walker, M. 1991. In Proceedings of the Fourth International Symposium on the Reproductive Physiology of Fish, 91, p. 328. Ed. by A.P. Scott, J.P. Sumpter, D.E. Kime, and M.S. Rolfe. FishSymp, Sheffield, Norwich.

Wood, S.N. 2006. Generalized Additive Models: An Introduction with R. Chapman & Hall/CRC, 392pp. Taylor and Francis Group, Boca Raton.

Wood, S.N., Pya, N., and Säfken, B. 2016. Smoothing parameter and model selection for general smooth models. Journal of the American Statistical Association, 111: 1548–1563.

Handling editor: Valerio Bartolino